EFFECTS OF GASEOUS SLIP FLOW AND TEMPERATURE JUMP ON ENTROPY GENERATION RATE IN RECTANGULAR MICRODUCTS

by

Abuzar GHAFFARI[a*], Waqar Ahmed KHAN[b], and Irfan MUSTAFA[c]

[a] Department of Mathematics, University of Education, Lahore, Attock Campus, Pakistan
[b] Department of Mechanical Engineering, College of Engineering, Prince Mohammad Bin Fahd University, Al Khobar, Kingdom of Saudi Arabia
[c] Department of Mathematics, Allama Iqbal Open University, H-8, Islamabad, Pakistan

Original scientific paper
https://doi.org/10.2298/TSCI181115029G

In this study, the influence of slip flow and temperature jump on the entropy generation rate are investigated in rectangular microducts. The Knudsen numbers are considered in the range between 0.001 and 0.1, and the aspect ratio lies between 0 and 1. The dimensionless governing equations are solved numerically using Chebyshev spectral collocation method, and the dimensionless velocity and temperature gradients are employed in the entropy generation model. The influences of the dimensionless numbers including Bejan number and irreversibility distribution ratio on the entropy generation rates are investigated and discussed through surface plots and contour diagrams. It is demonstrated that the minimum entropy generation rate exists corresponding to an optimal aspect ratio for each dimensionless number. This minimum entropy generation rate depends upon the nature of dimensionless numbers.

Key words: *Knudsen number, Bejan number, entropy generation rate, irreversibility, microducts, slip flow*

Introduction

Enhancement in the overall performance in different mechanical and engineering process always been the topic of interest for the engineers and scientists. Still, no such equipment has launched which convert the input energy into the valuable body of work without any loss. However, these losses can be minimized to get maximum overall performance. Various techniques are available to minimize these losses. However, the best practical method, to get the optimized results in thermodynamically systems, is the use of entropy generation minimization. Entropy generation is the primary concern in different engineering equipment like energy storage systems, geophysical fluid dynamics, heat exchangers and cooling of electronic devices. Gouy-Stodola in his theorem states that the rate of loss of exergy (irreversibility) is proportional to the entropy generation. However, method of entropy generation minimization (EMG) was first discussed by the Bejan [1]. According to him, the energy loss of thermodynamic systems can be controlled if the factors which cause the irreversibility can be

* Corresponding author, e-mails: abuzar.iiui@gmail.com; abuzar.ghaffari@ue.edu.pk

controlled, and thermodynamic optimization of the system can be attained. Minimization of entropy generation enhances the efficiency of a thermal system and leads to the reduction of the energy lost. That is for input energy to get maximum work done. The method of EGM is well described by Bejan [2-4] for the optimized results in various thermal systems. Carrington *et al*. [5] performed the entropy analysis in heat and mass transfer. The established a control volume solution for their model, and they consider in internal and external flows for heat and mass to apply this phenomenon to validate their findings. Nag *et al*. [6] carried out second law analysis through a duct assuming constant heat flux at the wall. They found that entropy generation during the process is directly proportional to lose in available energy and entropy generation can be minimized for an optimal value of the initial temperature difference. Sahin [7], considered various duct geometries to study the irreversibilities by assuming the constant heat flux at the wall. Demirel *et al*. [8] performed entropy analysis through a rectangular duct filled with spherical particles. They also assumed fluxes at the top (heated) and bottom (cooled) wall and calculated irreversibility distribution and entropy generation. Tasnim *et al.* [9] performed rational analysis inside two parallel isothermal plates placed in vertical direction saturated in a porous medium. They assumed that magnetic force is acting in transverse direction and expression of irreversibility distribution ratio and entropy generation number is also calculated analytically. Hooman [10] *et al.* performed first and the second law analysis through a rectangular duct saturated with porous medium and results are found analytically. Further notable studies [11-21] on entropy analysis are also carried in various geometries.

Study of fluid-flow and heat transfer rate through microscale has received much importance owing to their vast applications in chemical separation, micro-thermal technology, micro-propulsion, inkjet printheads, cooling of computer chips and in the field of biomedical. At microscopic scale (100 microns, *etc.*) and low pressure, gaseous flow does not follow the law continuum physics. In this situation, fluid velocity and temperature near the solid boundaries is different from an actual temperature of the boundaries. In the literature, this phenomenon is commonly known as velocity slip and thermal slip (temperature jumps), which is the primary source of change in flow characteristics.

The studies in the micro-channel with slip flow and temperature jumps have been carried out by most of the researches [22-29], and they carried out useful findings. Hooman [30] performed entropy analysis under various boundary conditions through duct geometry and used a numerical technique. He concluded that heating for the flow of gases through microducts of rectangular cross-section are essential and can change heat transfer. However, the study of entropy generation in rectangular microducts with the gaseous slip and temperature jumps has not been considered yet. Our present investigation majorly emphasizes on entropy generation minimization under velocity slip, and temperature jumps in microducts. A study is performed numerically by using spectral method and results are obtained for different emerging parameters.

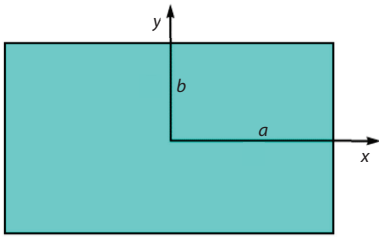

Figure 1. Schematic diagram

Mathematical formulation

Consider a rectangular duct whose semi major and minor axes are taken as a and b along x- and y-axes, fig. 1. The aspect ratio is $\varepsilon = b/a$. The gas is assumed to flow along z-axis. The governing equations for the flow and heat transfer in a microduct can be written:

– momentum equation

$$\frac{\partial^2 u}{\partial x^2}+\frac{\partial^2 u}{\partial y^2}=\frac{1}{\mu}\left(\frac{\partial p}{\partial z}\right) \tag{1}$$

– energy equation

$$\frac{\partial^2 T}{\partial x^2}+\frac{\partial^2 T}{\partial y^2}=\frac{1}{\alpha}u\left(\frac{\partial T}{\partial z}\right) \tag{2}$$

– subjected to fluid-flow conditions at the boundary

$$\begin{aligned} u &= -\lambda\frac{2-\sigma}{\sigma}\frac{\partial u}{\partial y} \quad \text{at} \quad y=b\,,\ 0\le x<a \\ u &= -\lambda\frac{2-\sigma}{\sigma}\frac{\partial u}{\partial x} \quad \text{at} \quad x=a\,,\ 0\le y<b \\ \frac{\partial u}{\partial y} &= 0 \quad \text{at} \quad y=0\,,\ 0\le x\le a \\ \frac{\partial u}{\partial x} &= 0 \quad \text{at} \quad x=0\,,\ 0\le y\le b \end{aligned} \tag{3a}$$

– and temperature jump conditions are

$$\left.\begin{aligned} T-T_w &= -\frac{\lambda}{\mathrm{Pr}}\frac{2-\sigma_t}{\sigma_t}\frac{2\gamma}{1+\gamma}\frac{\partial T}{\partial y} \quad \text{at} \quad y=b\,,\ 0\le x<a \\ T-T_w &= -\frac{\lambda}{\mathrm{Pr}}\frac{2-\sigma_t}{\sigma_t}\frac{2\gamma}{1+\gamma}\frac{\partial T}{\partial x} \quad \text{at} \quad x=a\,,\ 0\le y<b \end{aligned}\right\} \text{temperature jump conditions}$$

$$\left.\begin{aligned} \frac{\partial T}{\partial y} &= 0 \quad \text{at} \quad y=0\,,\ 0\le x\le a \\ \frac{\partial T}{\partial x} &= 0 \quad \text{at} \quad x=0\,,\ 0\le y\le b \end{aligned}\right\} \text{symmetry conditions} \tag{3b}$$

where u is the fluid velocity, T – the fluid temperature, α – the thermal diffusivity, σ – the tangential momentum accommodation coefficient, σ_t – thermal accommodation coefficient, λ – the molecular means free path, γ – the specific heat ratio, and Pr – the Prandtl number.

– using following transformations

$$\xi=\frac{x}{a},\ \eta=\frac{y}{b},\ \ w=\frac{u}{u_m p} \ \text{ and } \ T-T_w=\left(\frac{Q\,p}{k_f}\right)\theta \tag{4}$$

where

$$u_m=\frac{1}{A}\int_A w\,\mathrm{d}A,\ \ p=-\frac{b^2}{u_m\mu}\frac{\mathrm{d}p}{\mathrm{d}z},\ \ \frac{\mathrm{d}T}{\mathrm{d}z}=\frac{Q}{4ab\rho c_p u_m} \tag{5}$$

we get the following dimensionless forms for both momentum and energy equations:

$$\varepsilon^2\frac{\partial^2 w}{\partial\xi^2}+\frac{\partial^2 w}{\partial\eta^2}=-1 \tag{6}$$

$$\varepsilon^2 \frac{\partial^2 \theta}{\partial \xi^2} + \frac{\partial^2 \theta}{\partial \eta^2} = \frac{1}{4} \varepsilon w \tag{7}$$

– with dimensionless boundary conditions

$$\begin{aligned} u &= -\frac{4\mathrm{Kn}}{1+\varepsilon} \frac{2-\sigma}{\sigma} \frac{\partial u}{\partial \eta} \quad \text{at} \quad \eta = 1\,, \quad 0 \le \xi < 1 \\ u &= -\frac{4\varepsilon}{1+\varepsilon} \frac{2-\sigma}{\sigma} \frac{\partial u}{\partial \xi} \quad \text{at} \quad \xi = 1\,, \quad 0 \le \eta < 1 \\ \frac{\partial u}{\partial \eta} &= 0 \quad \text{at} \quad \eta = 0\,, \quad 0 \le \xi \le 1 \\ \frac{\partial u}{\partial \xi} &= 0 \quad \text{at} \quad \xi = 0\,, \quad 0 \le \eta \le 1 \end{aligned} \tag{8a}$$

where Kn is Knudsen number and it can be defied as the ratio of the molecular mean free path length to the characteristic length.

The dimensionless temperature at the boundary of the duct:

$$\left.\begin{aligned} \theta &= -\frac{2-\sigma_t}{\sigma_t} \frac{4}{1+\varepsilon} \frac{\mathrm{Kn}}{\mathrm{Pr}} \frac{2\gamma}{1+\gamma} \frac{\partial \theta}{\partial \eta} \quad \text{at} \quad \eta = 1\,, \quad 0 \le \xi < 1 \\ \theta &= -\frac{2-\sigma_t}{\sigma_t} \frac{4\varepsilon}{1+\varepsilon} \frac{\mathrm{Kn}}{\mathrm{Pr}} \frac{2\gamma}{1+\gamma} \frac{\partial \theta}{\partial \xi} \quad \text{at} \quad \xi = 1\,, \quad 0 \le \eta < 1 \end{aligned}\right\} \text{temperature jump conditions}$$

$$\left.\begin{aligned} \frac{\partial \theta}{\partial \eta} &= 0 \quad \text{at} \quad \eta = 0\,, \quad 0 \le \xi \le 1 \\ \frac{\partial \theta}{\partial \xi} &= 0 \quad \text{at} \quad \xi = 0\,, \quad 0 \le \eta \le 1 \end{aligned}\right\} \text{symmetry conditions} \tag{8b}$$

Entropy generation analysis

Following Bejan [1], the entropy generation rate in ducts can be written:

$$S_G = \overbrace{\frac{k_f}{T_0^2}\left[\left(\frac{\partial T}{\partial x}\right)^2 + \left(\frac{\partial T}{\partial y}\right)^2 + \left(\frac{\partial T}{\partial z}\right)^2\right]}^{\text{Entropy generation due to heat transfer } S_{G,h}} + \overbrace{\frac{\mu}{T_0}\left[\left(\frac{\partial u}{\partial x}\right)^2 + \left(\frac{\partial u}{\partial y}\right)^2\right]}^{\text{Entropy generation due to fluid friction } S_{G,f}} \tag{9}$$

To develop its dimensionless form, we used eqs. (3) and (4) and got the following:

$$\begin{aligned} S_G = \frac{k_f}{T_0^2}\left[\left(\frac{1}{a}\frac{Q\,p}{k_f}\theta_\xi\right)^2 + \left(\frac{1}{b}\frac{Q\,p}{k_f}\theta_\eta\right)^2 + \left(\frac{Q}{4ab\rho c_p u_m}\right)^2\right] + \\ + \frac{\mu}{T_0}\left[\left(\frac{u_m p}{a} w_\xi\right)^2 + \left(\frac{u_m p}{b} w_\eta\right)^2\right] \end{aligned} \tag{10}$$

$$S_G = \frac{Q^2 p^2}{T_0^2 b^2 k_f}\left[\varepsilon^2\theta_\xi^{\,2} + \theta_\eta^{\,2} + \left(\frac{\varepsilon}{4}\right)^2\left(\frac{k_f}{bp}\frac{1}{\rho c_p u_m}\right)^2\right] + \frac{\mu}{T_0}\frac{u_m^{\,2}p^2}{b^2}\left[\varepsilon^2 w_\xi^{\,2} + w_\eta^{\,2}\right] \tag{11}$$

$$N_s = \frac{S_G}{S_{G_0}} = \varepsilon^2\theta_\xi^{\,2} + \theta_\eta^{\,2} + \left(\frac{\varepsilon}{4}\right)^2\left(\frac{k_f}{bp}\frac{1}{\rho c_p u_m}\right)^2 + \frac{\mu}{T_0}\frac{u_m^{\,2}k_f T_0}{Q^2}\left[\varepsilon^2 w_\xi^{\,2} + w_\eta^{\,2}\right] \tag{12}$$

where

$$S_{G_0} = \frac{Q^2 p^2}{T_0^2 b^2 k_f}$$

$$N_s = \overbrace{\varepsilon^2\theta_\xi^{\,2} + \theta_\eta^{\,2} + \left(\frac{\varepsilon}{4}\right)^2\left(\frac{1}{\mathrm{Pe}}\right)^2}^{Ns_h} + \overbrace{\frac{\mathrm{Br}}{\omega}\left[\varepsilon^2 w_\xi^{\,2} + w_\eta^{\,2}\right]}^{Ns_f} \tag{13}$$

where

$$\mathrm{Pe} = \mathrm{Re}\,\mathrm{Pr} = \frac{(\rho u_m)b}{\nu}\frac{\nu}{\alpha} = \frac{(\rho u_m)b}{\alpha},\ \mathrm{Br} = \frac{\mu u_m^2}{Q},\ \omega = \frac{\Delta T}{T_0},\ \Delta T = \frac{Q}{k_f}$$

In the aforementioned equation, the term Ns_h is the heat transfer irreversibility and Ns_h – the fluid friction irreversibility. Bejan number is the ratio of heat transfer irreversibility to the total irreversibility and can be written:

$$\mathrm{Be} = \frac{Ns_h}{N_s} = \frac{Ns_h}{Ns_h + Ns_f} = \frac{1}{1 + \dfrac{Ns_f}{Ns_h}} = \frac{1}{1+\Phi} \tag{14}$$

where $\Phi = Ns_f/Ns_h$ is the irreversibility distribution ratio. From eq. (13), it is inferred that the Bejan number lies between 0 and 1. When Be = 1, heat transfer irreversibility dominates over fluid friction irreversibility, whereas Be = 0 confirms the dominance of fluid friction irreversibility over heat transfer irreversibility. When Be = 0.5, both heat transfer and friction irreversibilities are equally dominant.

Results and discussion

The obtained system of dimensionless eqs. (6)-(8) is simulated through Chebyshev spectral collocation scheme, accurate up to 10^{-6}. The domain $0 \le \xi < 1$ and $0 \le \eta < 1$ is transformed to $-1 \le \xi < 1$ and $-1 \le \eta < 1$ using the formula $\xi = 2\eta/(L-1)$. The node points between 1 and –1 are calculated by using the formula $\xi j = \cos(\pi j/N)$, $j = 0, 1, 2, \ldots N$ and $\eta i = \cos(\pi i/N)$, $i = 0, 1, 2, \ldots N$ along ξ and η direction, respectively. The equal number of node points are considered in both directions. These node points are commonly known as Gauss-Lobatto collocation points. The obtained results are presented through the figs. 2-9, while the value of the parameter $\sigma_t = \sigma = 1$ is kept fix and others are mentioned corresponding to each figure. The variation of several entropy generation rates with the aspect ratio is displayed in figs. 2-4 for different dimensionless numbers including Peclet, Brinkman, and Knudsen numbers keeping other parameters fixed. In each case, the entropy generation rate due to heat transfer irreversibility is decreasing, whereas, the entropy generation rate due to fluid friction irreversibility is increasing with aspect ratio for each dimensionless number. Also, there is a minimum entropy generation rate corresponding to an optimal aspect ratio for each dimensionless number.

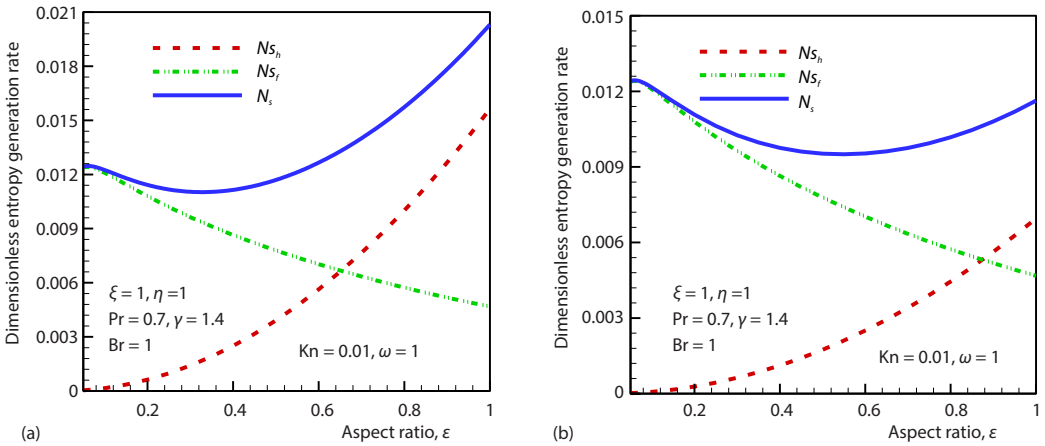

Figure 2. Variation of dimensionless entropy generation rates with aspect ratio when (a) Pe = 2, (b) Pe = 3

This minimum entropy generation rate depends upon the nature of dimensionless numbers. The Peclet number establishes the relation between conducted and convected thermal energy to the fluid. The larger the Peclet number, the larger will be the convected thermal energy to the fluid. This is confirmed in figs. 2(a) and 2(b) for two different Peclet numbers. The Brinkman number demonstrates the relation between viscous heat generation and external heating. It increases with an increase in viscous dissipation and as a result the minimum entropy generation rate increases with Brinkman number. This can be observed in figs. 3(a) and (b). The same fact can be observed in figs. 4(a)-4(d) for increasing values of Knudsen numbers in the slip flow regime ($0.01 \leq \mathrm{Kn} \leq 0.1$). The variation of entropy generation rates and Bejan number along axial and transverse directions are shown in surface plots, see figs. 5(a)-5(d). The isotherms for the same quantities are shown in figs. 6 and 7 for the fixed parameters. The isotherms of entropy generation rate due to heat and fluid friction are displayed in figs. 6(a) and 6(b), respectively for Kn = 0.1. The variation in magnitude with the position

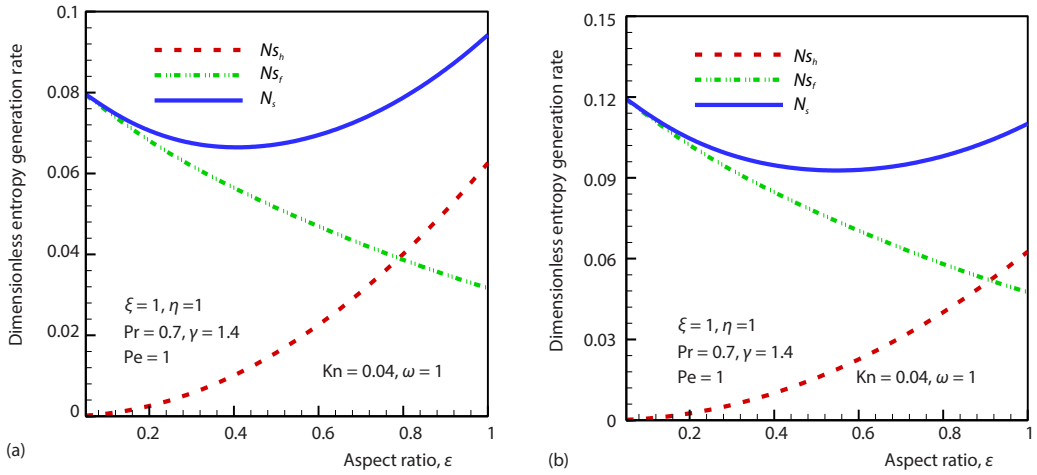

Figure 3. Variation of dimensionless entropy generation rates with aspect ratio when (a) Br = 1, (b) Br = 1.5

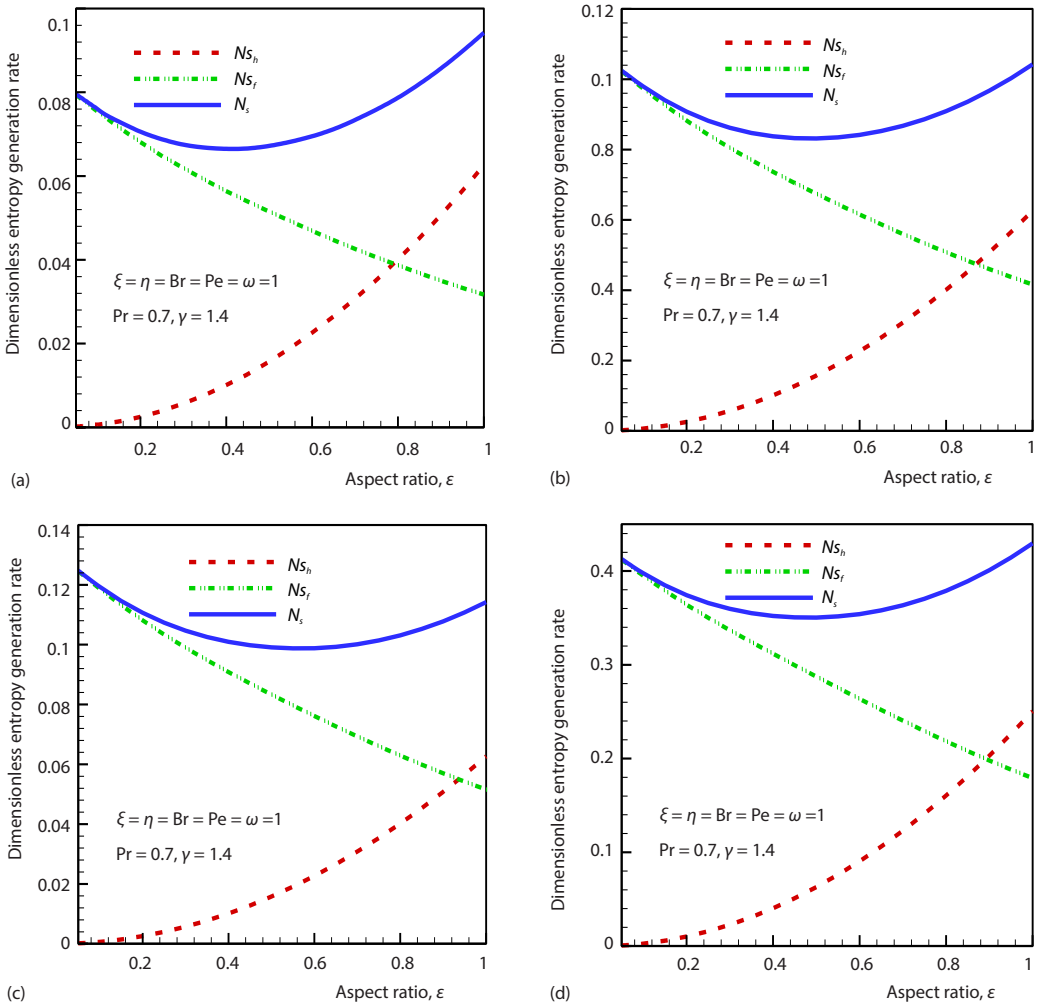

Figure 4. Variation of dimensionless entropy generation rates with aspect ratio when (a) Kn = 0.04, (b) Kn = 0.05, (c) Kn = 0.06, and Kn = 0.1

exhibits the distribution of irreversibilities due to heat and fluid friction. It is observed that the effect of fluid friction irreversibility is dominant near the left and top surfaces of the duct.

On the other side, the fluid friction irreversibility shows minimum contribution. Similarly, contours of total entropy generation rate and Bejan numbers are shown in figs. 7(a) and 7 (b), respectively. Figure 7(a) demonstrates that the total entropy generation inside the duct is practically the same as the entropy generation due to fluid friction.

Figures 8(a) and 8(b) display the variation of Bejan number with aspect ratios for different values of Knudsen and Peclet numbers, respectively. The behavior of Bejan numbers is found to be the same in both cases. In case of parallel plate channel when $\varepsilon \rightarrow 0$ the irreversibility due to fluid friction is higher and as the aspect ratio increases to the square duct, the irreversibility due to heat transfer increases and both irreversibilities become comparable depending upon the values of Knudsen and Peclet numbers. In both cases, the Bejan number decreases with increasing Knudsen or Peclet numbers for the square duct. The Second law of

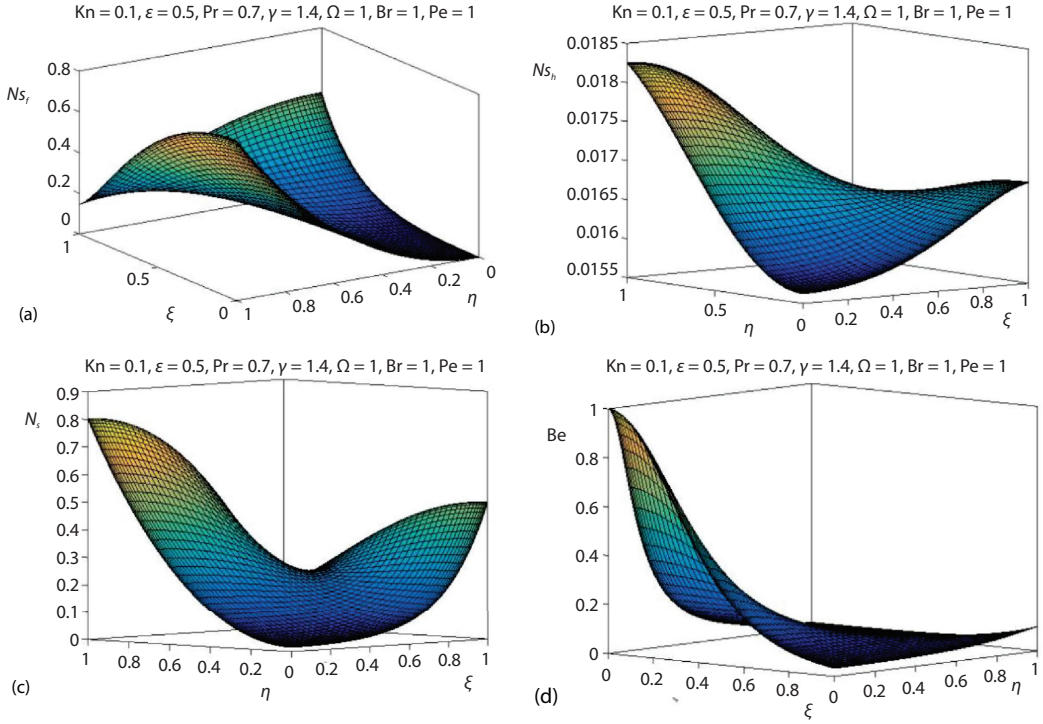

Figure 5. Surface plots for (a) entropy generation rate due to fluid friction, (b) entropy generation rate due to heat, (c) total entropy generation rate, and (d) Bejan number

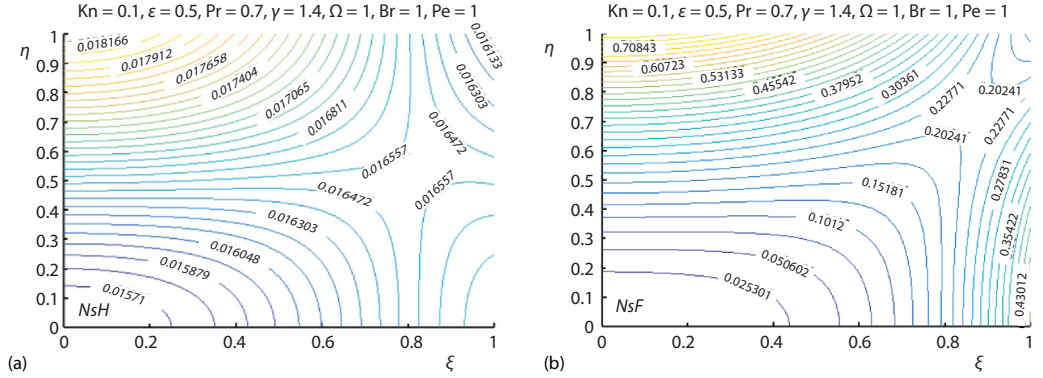

Figure 6. Entropy generation contours in a microduct due to (a) heat irreversibility, (b) fluid friction reversibility

thermodynamics combines the irreversibility due to fluid friction and heat transfer. In all thermal systems, the entropy changes due to these irreversibilities. The higher the irreversibility due to fluid friction, the higher will be the irreversibility distribution ratio. Figures 9(a) and 9(b) demonstrate the variation of irreversibility distribution ratio with aspect ratio for different values of Knudsen and Peclet numbers, respectively. In both cases, the irreversibility due to friction is higher for smaller aspect ratios and decreases with increasing Knudsen or Peclet numbers. For square ducts, both irreversibilities due to fluid friction and heat transfer are found to be equivalent.

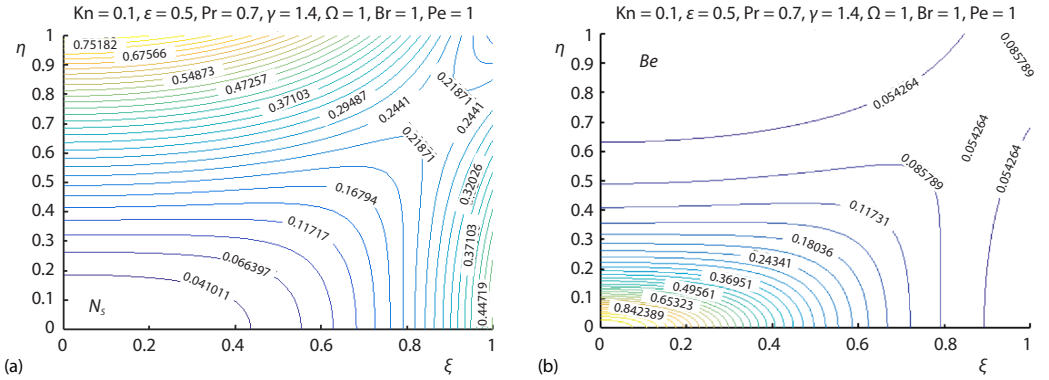

Figure 7. (a) Contours for total entropy generation rate, (b) Bejan number contours in a microduct

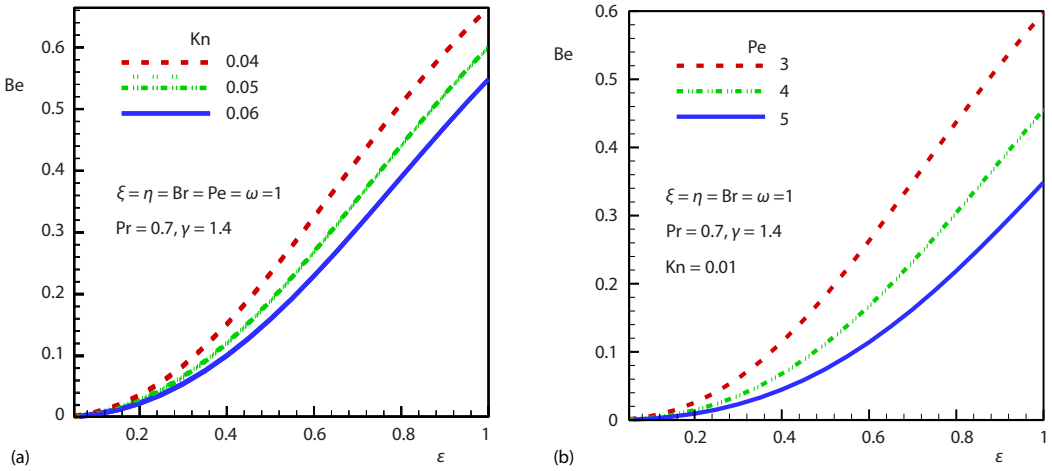

Figure 8. Variation of Bejan number with aspect ratio for different values of (a) Kn, (b) Pe

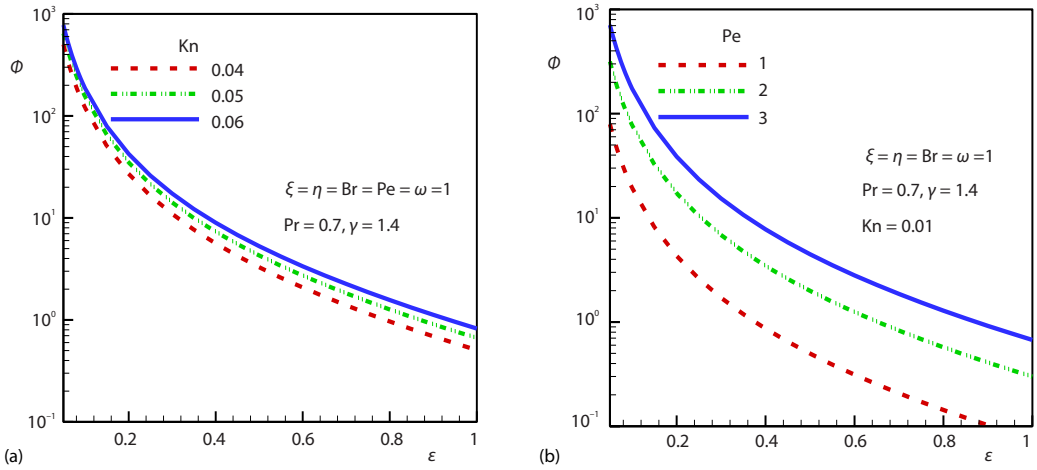

Figure 9. Variation of irreversibility distribution ratio with aspect ratio for different values of (a) Kn, (b) Pe

Conclusions

In this study, a model for the total entropy generation rate is developed for rectangular microducts. The Knudsen numbers are considered in the range between 0.001 and 0.1, and the aspect ratio lies between 0 and 1. The main results are summarized as follows.

- The entropy generation rate due to heat transfer irreversibility decreases, whereas, the entropy generation rate due to fluid friction irreversibility increases with aspect ratio.
- The minimum entropy generation rate exists corresponding to an optimal aspect ratio in each case.
- The fluid friction irreversibility is dominant near the left and top surfaces of the duct.
- In the case of a parallel plate channel, the irreversibility due to fluid friction is higher.
- The irreversibility distribution ratio decreases with aspect ratio for different dimensionless numbers.

Nomenclature

A – cross-sectional area, [L^2]
a – long length of microchannel, [L]
b – short length of microchannel, [L]
Be – Bejan number, [–]
Br – Brinkman number, [–]
Kn – Knudsen number, [–]
N_s – total entropy generation rate, [$ML^2T^{-2}K^{-1}$]
Ns_f – entropy generation rate due to fluid friction, [$ML^2T^{-2}K^{-1}$]
Ns_h – entropy generation rate due to heat, [$ML^2T^{-2}K^{-1}$]
Pe – Peclet number, [–]
p – pressure, [$ML^{-1}T^{-2}$]
T – fluid temperature, [K]
u – fluid velocity, [LT^{-1}]
u_m – average fluid velocity, [LT^{-1}]
w – fluid velocity in dimensionless form, [–]

Greek symbols

α – thermal diffusivity, [L^2T^{-1}]
ε – aspect ratio, [–]
θ – dimensionless temperature profile, [–]
λ – molecular mean free path, [L]
σ – tangential momentum accommodation coefficient, [–]
σ_t – thermal accommodation coefficient, [–]
γ – specific heat ratio, [–]
Φ – the irreversibility distribution ratio, [–]

References

[1] Bejan, A., *Entropy Generation Minimization*, CRC, New York, USA, 1996
[2] Bejan, A., Entropy Generation Minimization: The New Thermodynamics of Finite-Size Devices and Finite-Time Processes, *Journal of Applied Physics*, *79* (1996), 3, pp. 1191-1218
[3] Bejan, A., Thermodynamic Optimization of Geometry in Engineering Flow Systems, Exergy, an International Journal, *1* (2001), 4, pp. 269-277
[4] Bejan, A., Fundamentals of Exergy Analysis, Entropy Generation Minimization, and the Generation of Flow Architecture, *International Journal of Energy Research*, *26* (2002), 7, pp. 545-565
[5] Carrington, C. G., *et al*., Second Law Analysis of Combined Heat and Mass Transfer in Internal and External Flows, *International Journal of Heat and Fluid-Flow*, *13* (1992), 1, pp. 65-70
[6] Nag, P. K., *et al*., Second Law Optimization of Convective Heat Transfer through a Duct with Constant Heat Flux, *International Journal of Energy Research*, *13* (1989), 5, pp. 537-543
[7] Sahin, A. Z., Irreversibilities in Various Duct Geometries with Constant Wall Heat Flux and Laminar Flow, *Energy*, *23* (1998), 6, pp. 465-473
[8] Demirel, Y., *et al*., Entropy Generation in a Rectangular Packed Duct with Wall Heat Flux, *International Journal of Heat and Mass Transfer*, *42* (1999), 13, pp. 2337-2344
[9] Tasnim, S. H., *et al*., Entropy Generation in a Porous Channel with Hydromagnetic Effect, *Exergy*, *An International Journal*, *2* (2002), 4, pp. 300-308
[10] Hooman, K., *et al*., Heat Transfer and Entropy Generation Optimization of Forced Convection in a Porous-Saturated Duct of Rectangular Cross-Section, *International Journal of Heat and Mass Transfer*, *50* (2007), 11-12, pp. 2051-2059
[11] Hooman, K., *et al.*, Analysis of Heat Transfer and Entropy Generation for a Thermally Developing Brinkman-Brinkman Forced Convection Problem in a Rectangular Duct with Isoflux Walls, *International Journal of Heat and Mass Transfer*, *50* (2007), 21-22, pp. 4180-4194

[12] Yadav, S. L., *et al.,* Ashok Kumar Singh, Analysis of Entropy Generation in a Rectangular Porous Duct, *Journal of Applied Mathematics and Physics*, *4* (2016), 7, pp. 1336-1343
[13] Silva, R.L., *et al.*, Temperature and Entropy Generation Behavior in Rectangular Ducts with 3-D Heat Transfer Coupling (Conduction and Convection), *International Communications in Heat and Mass Transfer*, *35* (2008), 3, pp. 240-250
[14] Oztop, H. F., *et al.*, Entropy Generation through Hexagonal Cross-Sectional Duct for Constant Wall Temperature in Laminar Flow, *International Journal of Energy Research*, *28* (2004), 8, pp. 725-737
[15] Sahin, A. Z., *et al.*, A Simple Method of Determining Entropy Generation Rate in Viscous Fluid-Flow through Ducts, *Arabian Journal for Science and Engineering, 39* (2014) 2, pp. 1241-1249
[16] Ko, T. H., *et al.*, Entropy Generation and Optimal Analysis for Laminar Forced Convection in Curved Rectangular Ducts: A Numerical Study, *International Journal of Thermal Sciences*, *45* (2006), 2, pp. 138-150
[17] Ko, T. H., Numerical Investigation on Laminar Forced Convection and Entropy Generation in a Curved Rectangular Duct with Longitudinal Ribs Mounted on Heated Wall, *International Journal of Thermal Sciences*, *45* (2006), 4, pp. 390-404
[18] Cheng, K. C., *et al.*, Laminar Forced Convection Heat Transfer in Curved Rectangular Channels, *International Journal of heat and mass Transfer*, *13* (1970), 3, pp. 471-490
[19] Esfahani, J. A., *et al.*, Accuracy Analysis of Predicted Velocity Profiles of Laminar Duct Flow with Entropy Generation Method, *Applied Mathematics and Mechanics*, *34* (2013), 8, pp. 971-984
[20] Wu, S. Y., *et al.,* Exergy Transfer Characteristics of Forced Convective Heat Transfer through a Duct with Constant Wall Temperature, *Energy*, *32* (2007), 12, pp. 2385-2395
[21] Hooman, K., Entropy Generation for Microscale Forced Convection: Effects of Different Thermal Boundary Conditions, Velocity Slip, Temperature Jump, Viscous Dissipation, and Duct Geometry, *International Communications in Heat and Mass Transfer*, *34* (2007), 8, pp. 945-957
[22] Ghodoossi, L., Prediction of Heat Transfer Characteristics in Rectangular Micro-Channels for Slip Flow Regime and H1 Boundary Condition, *International Journal of Thermal Sciences*, *44* (2005), 6, pp. 513-520
[23] Khan, W. A., *et al.*, Optimization of Micro-Channel Heat Sinks Using Entropy Generation Minimization Method,*T wenty-Second Annual IEEE Semiconductor Thermal Measurement And Management Symposium, 32* (2006), 2, pp. 78-86
[24] Duan, Z., *et al.*, Slip Flow in Non-Circular Micro-Channels, *Micro-Fluidics and Nanofluidics*, *3* (2007), 4, pp. 473-484
[25] Gorla, R. S. R., *et al.*, Second Law Analysis for Microscale Flow and Heat Transfer, *Applied Thermal Engineering*, *27* (2007), 8-9, pp. 1414-1423
[26] Ebrahimi, A., *et al.*, Heat Transfer and Entropy Generation in a Micro-Channel with Longitudinal Vortex Generators Using Nanofluids, *Energy*, *101* (2016), Apr., pp. 190-201
[27] Awad, M. M., A Review of Entropy Generation in Micro-Channels, *Advances in Mechanical Engineering*, *7* (2015), 12, pp. 1-32
[28] Kuddusi, L., Entropy Generation in Rectangular Micro-Channels, *International Journal of Exergy*, *19* (2016), 1, pp. 110-139
[29] Baghani, M., *et al.*, Gaseous Slip Flow Forced Convection in Microducts of Arbitrary but Constant Cross-Section, *Nanoscale and Microscale Thermophysical Engineering*, *18* (2014) 4, pp. 354-372
[30] Hooman, K., Heat Transfer and Entropy Generation for Forced Convection through a Microduct of Rectangular Cross-Section: Effects of Velocity Slip, Temperature Jump, and Duct Geometry, *International Communications in Heat and Mass Transfer*, *35* (2008), 9, pp. 1065-1068

Paper submitted: November 15, 2018
Paper revised: January 7, 2019
Paper accepted: January 11, 2019